Critical Determinants of Uptake and Translocation of Nanoparticles by the Human Pulmonary Alveolar Epithelium

Andrew J. Thorley,[*,†,§] Pakatip Ruenraroengsak,[†,‡,§] Thomas E. Potter,[†] and Teresa D. Tetley[*,†]

[†]Lung Cell Biology, Section of Pharmacology and Toxicology, National Heart and Lung Institute, Imperial College London, London SW3 6LY, U.K. and [‡]Department of Materials and London Centre for Nanotechnology, Imperial College London, Exhibition Road, London SW7 2AZ, U.K. [§]These authors contributed equally.

ABSTRACT The ability to manipulate the size and surface properties of nanomaterials makes them a promising vector for improving drug delivery and efficacy. Inhalation is a desirable route of administration as nanomaterials preferentially deposit in the alveolar region, a large surface area for drug absorption. However, as yet, the mechanisms by which particles translocate across the alveolar epithelial layer are poorly understood. Here we show that human alveolar type I epithelial cells internalize nanoparticles, whereas alveolar type II epithelial cells do not, and that nanoparticles translocate across the epithelial monolayer but are unable to penetrate the tight junctions between cells, ruling out paracellular translocation. Furthermore, using siRNA, we demonstrate that 50 nm nanoparticles enter largely by passive diffusion and are found in the cytoplasm, whereas 100 nm nanoparticles enter primarily *via* clathrin- and also caveolin-mediated endocytosis and are found in endosomes. Functionalization of nanoparticles increases their uptake and enhances binding of surfactant which further promotes uptake. Thus, we demonstrate that uptake and translocation across the pulmonary epithelium is controlled by alveolar type I epithelial cells, and furthermore, we highlight a number of factors that should be considered when designing new nanomedicines in order to improve drug delivery to the lung.

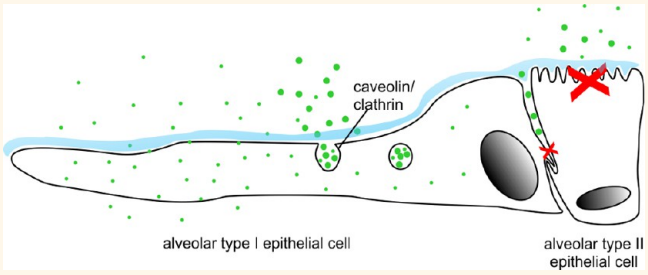

KEYWORDS: human · epithelial · siRNA · endocytosis · nanoparticles · surfactant · lung

In the past decade, there has been a remarkable increase in the development and use of nanomaterials in a wide variety of industries.[1] Their use in medicine as delivery vehicles is particularly promising, as manipulation of the particle's size and surface properties can optimize drug delivery and target specific organs.[2−5] One desirable route of nanomedicine delivery is through inhalation; a high percentage of inhaled nanomaterials preferentially deposit in the respiratory, alveolar region,[6] the epithelial layer of which covers approximately 150 m^2 and thus represents a large surface area for nanoparticle uptake and potential translocation to the pulmonary interstitium and cardiovasculature.

The alveolar epithelium consists of two epithelial cell types, cuboidal alveolar type II epithelial (ATII) cells and flattened alveolar type I epithelial (ATI) cells. Although ATII cells outnumber ATI cells 2:1, the large, attenuated ATI cells cover over 95% of the alveolar surface. Thus, these are a primary target of inhaled nanoparticles; ATI cells possess clathrin- and caveolin-mediated endocytic pathways[7] important in *trans*-epithelial transport, receptor recycling, and cellular signaling.[8] Secretory ATII cells synthesize and release pulmonary surfactant, a phospholipid-enriched fluid that reduces surface tension at the air−liquid interface and contains surfactant proteins A−D, which act as opsonins to promote microbial clearance. Previous studies have demonstrated that surfactant proteins can bind to air pollution particles,[9] and inhaled particles depositing on the surface of the surfactant layer are displaced toward the alveolar epithelial cell surface which may promote cellular uptake.[10] ATII cells also possess endocytic pathways for internalizing

* Address correspondence to andrew.thorley@imperial.ac.uk, t.tetley@imperial.ac.uk.

Received for review September 23, 2014 and accepted October 31, 2014.

Published online October 31, 2014
10.1021/nn505399e

and recycling used surfactant components *via* lamellar bodies.[11,12]

The primary mechanism for clearance of micron-sized foreign bodies is phagocytosis by resident alveolar macrophages. Smaller, individual, nanosized particles may not be recognized by macrophages and might instead be internalized by the alveolar epithelium. Previous *in vivo* and *in vitro* studies suggest that inhaled nanomaterials can penetrate epithelial cells[13] and traverse the alveolar epithelium and distribute systemically,[14] *via* endocytic pathways, as well as by passive nonenergy requiring mechanisms.

A number of *in vitro* studies have investigated cellular uptake of nanoparticles using a range of human carcinoma-derived cell lines and animal-derived cells in conjunction with pharmacological agents that inhibit endocytic pathways. Consequently, to date there is no clear understanding of the mechanisms that are involved in the transfer of nanoparticles across the human respiratory barrier. Thus, more robust techniques and physiologically relevant models are needed to fully understand the mechanisms by which inhaled nanoparticles and potential nanomedicines interact with the pulmonary epithelium; it is likely that a number of biological interactions will determine the route and degree of cellular uptake.

In this study, we take a systematic approach to investigating the nanobio interface within the alveolus using relevant *in vitro* models of primary human ATII cells and a unique transformed human ATI cell line (TT1) derived from normal human lung tissue.[15] Using high-resolution electron microscopy and mechanistic studies, we describe the effect of physicochemical properties of nanoparticles on epithelial cell uptake, how uptake differs between different alveolar epithelial cells within the human lung, and how native surfactant proteins can bind to nanoparticles and modify their uptake. Importantly, we have used siRNA to investigate which endocytic pathways were important by specific knockdown of proteins involved in clathrin and caveolin-mediated pathways; this approach avoids the potentially confounding broad spectrum effects of the more commonly used pharmacological inhibitors such as nocodazole and chlorpromazine.[16,17] Thus, this study provides an insight into factors that are likely to govern particle translocation across the gas−blood barrier and which should be considered when designing nanodrugs for pulmonary delivery.

RESULTS

We used two sizes of well-defined fluorescently labeled model polystyrene (PS) nanoparticles,[18] 50 and 100 nm, and three surface modifications, unmodified (unmodified PS), carboxyl-modified (carboxyl PS), and amine-modified (amine PS), to investigate the significance of size and surface modification on nanoparticle uptake by human alveolar epithelial cells.

Cell Specific Uptake of Nanoparticles. We discovered that there was a significant difference in nanoparticle uptake between TT1 cells and ATII cells 4 h after exposure. While TT1 cells internalized significant amounts of nanoparticles of all sizes and modifications, we were surprised to see that uptake of these nanoparticles by ATII cells was almost undetectable (Figure 1). These are unique observations, not previously performed by others, and are highly relevant in light of the 95% contribution of TTI cells to the alveolar surface area, suggesting that ATI cells will govern uptake and potential translocation of inhaled nanoparticles across the pulmonary epithelial barrier. Many previous studies have used A549 adenocarcinoma cell lines as a model of ATII cells to investigate nanoparticle uptake;[19−21] in light of the current findings and previous findings by us showing fundamental differences between A549 cells, TT1 cells, and primary ATII cells,[22,23] we suggest that A549 cells may not truly reflect how alveolar epithelial cells are likely to respond to nanoparticles *in vivo*. Thus, for all subsequent investigations of nanoparticle uptake by the alveolar epithelium, only TT1 cells were used.

Using fluorescence microscopy image analysis, we demonstrated that uptake of NPs by TT1 cells was size-, surface modification-, and time-dependent (Figure 2). 50 nm amine PS was internalized more rapidly and to a greater extent than unmodified PS and carboxyl PS (4 h; 6.4-fold and 2.2-fold, respectively; $P < 0.0001$). The rapid uptake of amine PS compared to other surface modifications is likely due to their higher affinity for the negatively charged surface of the cell membrane. Furthermore, by 4 h, uptake of 50 nm carboxyl PS was significantly greater than that of unmodified PS of the same size (2.9-fold; $P < 0.0001$). The increased uptake of functionalized 50 nm PS compared to unmodified PS may also be, in part, due to the wide array of moieties such as glycolipids, glycoproteins, and receptors found in the cell membrane that could provide electrostatic interaction sites for carboxyl and amine groups. We have previously demonstrated that the surface functionalization of 50 nm polystyrene nanoparticles has a significant effect on how they interact with the cell membrane of TT1 cells;[18] at concentrations higher than used in this study, amine PS are able to create holes in the membrane of TT1 cells whereas unmodified PS and carboxyl PS do not. This is despite the fact that, under the same culture conditions used in this study, the surface charge of unmodified PS, carboxyl PS, and amine PS is altered such that they all possess a similar charge of between −10 and −20 mV. We hypothesize that the alteration in particle charge due to adsorption of components of the cell culture medium may be dynamic such that the amine and carboxyl groups still confer a functional effect when the particles come in to contact with the cell membrane.

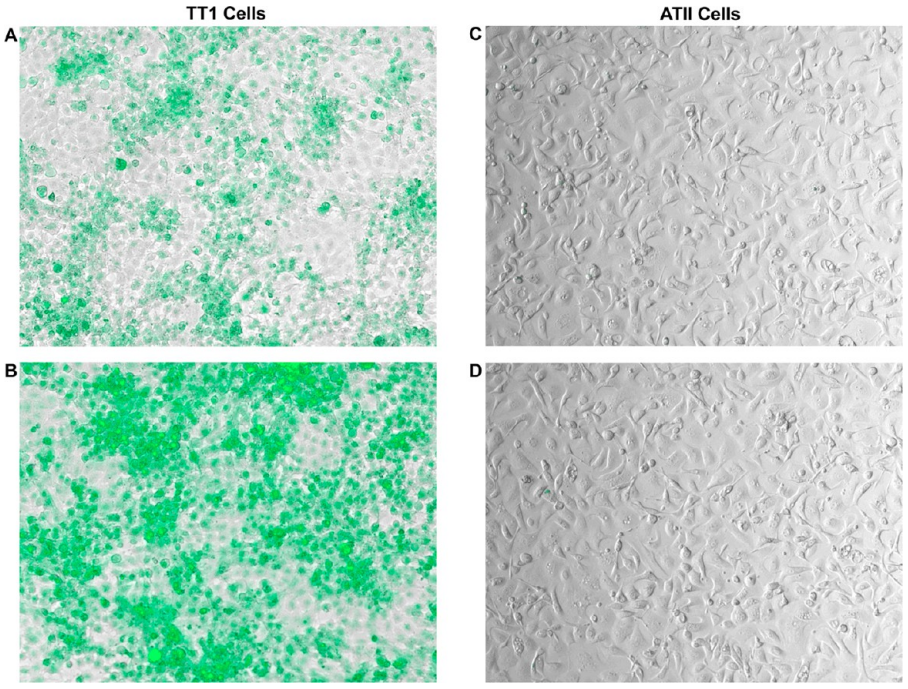

Figure 1. Cell-specific uptake of nanoparticles. Confluent monolayers of primary human alveolar type II epithelial (ATII) cells and TT1 cells were exposed to 50 nm nanoparticles for 4 h. Fluorescent microscopy demonstrated that ATII cells did not internalize unmodified PS (A) or carboxyl PS (B). On the contrary, TT1 cells avidly internalized unmodified PS (C) and carboxyl PS (D). The same was observed for 50 nm amine PS and equivalent 100 nm PS. Images representative of three separate experiments.

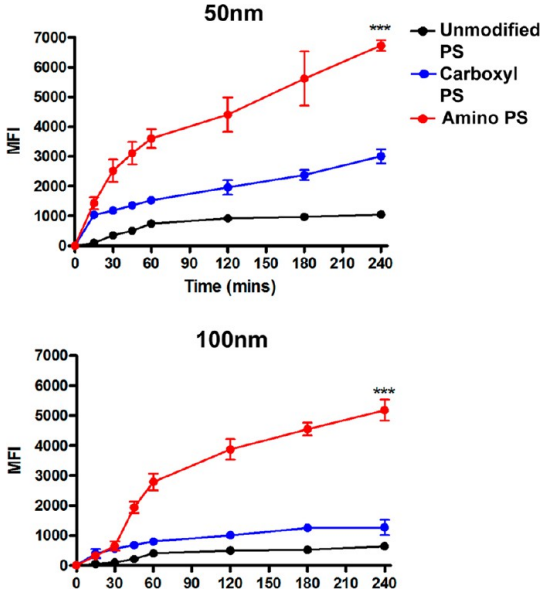

Figure 2. Uptake of nanoparticles by human TT1 cells is size and surface modification-dependent. TT1 cells internalized 50 nm polystyrene amine PS significantly faster and to a greater degree than carboxyl PS and unmodified PS. Similarly, 100 nm amine PS were internalized by TT1 cells to a greater degree than carboxyl PS and unmodified PS of the equivalent size; however, internalization of 100 nm NPs was significantly less than 50 nm nanoparticles of the corresponding surface modification. Data expressed as mean ± standard deviation, $n = 4$ experiments. ***$P < 0.0001$ amine PS vs unmodified PS; †† $P < 0.0001$ carboxyl PS vs unmodified PS.

The same hierarchy of uptake was also observed in studies using 100 nm nanoparticles (Figure 2), with the notable difference that significantly less of the 100 nm nanoparticles were internalized than 50 nm particles (4 h; $P < 0.002$). We hypothesize that the increased uptake of 50 nm nanoparticles compared to 100 nm nanoparticles is not only due to the decreased cellular energy required to internalize smaller particles, as previously demonstrated,[24] but also due to the ability of smaller nanoparticles to enter the cell *via* passive diffusion and endocytic pathways whereas larger nanoparticles enter largely *via* endocytosis alone.

Our observations are particularly interesting when the exposure system used in this study is considered. In submerged culture it could be hypothesized that colloidal behavior such as agglomeration, diffusion, and sedimentation rates may affect nanoparticle behavior such that 100 nm nanoparticles would sediment faster than 50 nm nanoparticles, and thus, the chance of interaction with the cell monolayer would be greater which could lead to a higher rate of internalization. However, we see a rapid internalization of 50 nm nanoparticles at 15 min which is significantly greater than equivalent 100 nm nanoparticles ($P < 0.005$) suggesting that sedimentation of nanoparticles is not a confounding factor when comparing the effect of size on nanoparticle uptake. A previous study by Limbach *et al.* investigated the effect of size and particle concentration on the uptake of ceria nanoparticles by human lung fibroblasts.[25] In this study, it was demonstrated that particle uptake was significantly affected by particle size such that larger nanoparticles (~320 nm)

were internalized more than smaller (~25 nm). It was hypothesized that this was due to the slow diffusion and increased agglomeration of small nanoparticles limiting uptake. However, comparing particles in two size ranges similar to that used in this study (50 and 100 nm), there was no significant size-dependent difference in uptake at concentrations above 10 μg/mL. While uptake was only measured after 10 min, this study supports our hypothesis that particle size was not a confounding factor in our study. In order to further investigate whether colloidal behavior affects nanoparticle uptake in submerged culture, future studies using aerosolized delivery of nanoparticles to TT1 cells grown at an air liquid interface (ALI) as a comparison would be of great benefit. Recent studies have shown that by using aerosolized delivery of nanoparticles to ALI cultures more physiologically relevant concentrations can be used to achieve functional readouts.[26]

Uptake and Translocation of Nanoparticles. The fate of nanoparticles internalized by the alveolar epithelium is unclear and has been hampered by the lack of robust *in vitro* models and difficulty in tracing nanoparticles *in vivo*. However, previous animal studies have demonstrated that polystyrene nanoparticles, and other types of nanoparticles, can translocate in to the systemic circulation,[27−29] albeit in low amounts; inhaled insulin particles have been developed for the treatment of diabetes with some success, suggesting pulmonary translocation not only occurs but may also be used for successful delivery of drugs to the systemic circulation.[30,31] Inhaled nanoparticles, deposited in the alveolar region, might enter the systemic circulation *via* uptake and translocation through epithelial cells or paracellularly *via* intercellular spaces, particularly if tight junctions are disrupted. To investigate this, we used transmission electron microscopy (TEM) to image TT1 cells exposed to polystyrene nanoparticles for 4 h. To date there have been no studies using TEM to spatially resolve the interaction of nanoparticles with human alveolar epithelial cells and how size and particle charge affect their cellular location. In studies where cells were exposed to nanoparticles for 4 h as before, we discovered a small proportion of nanoparticles located between the cells (Figure 3); however, they only reached as far as the apical side of intercellular tight junctions. This observation was seen with all particles, regardless of size and surface modification and suggests that these particles are unable to disrupt intercellular junctions and traverse the alveolar epithelial barrier *via* the paracellular route.

When cells were exposed to 50 nm nanoparticles, we observed numerous NPs distributed throughout the cytoplasm and, to a lesser extent, in vesicles (Figure 4), suggesting these particles entered by passive and active transport. In contrast, 100 nm nanoparticles, irrespective of modification were found primarily within

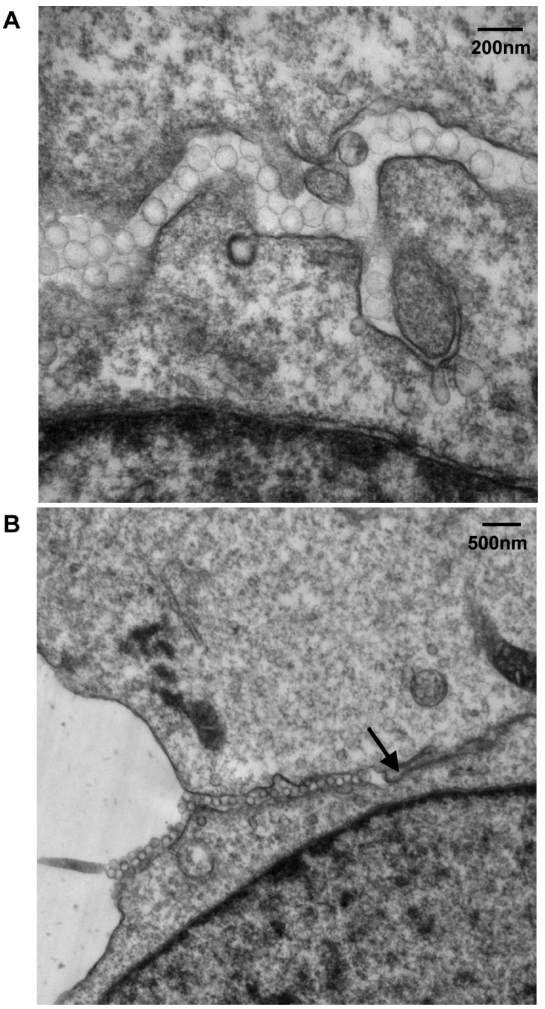

Figure 3. Paracellular distribution of NPs between TT1 cells. TT1 cells were imaged by TEM following 4 h exposure to 100 nm unmodified PS. 100 nm nanoparticles were observed in between the cells; (A) however, they only reached as far as the tight junction (B, black arrow) and were never observed beyond this point. This observation was the same for all sizes and surface modifications of NP.

intracellular vesicles, and very few were free in the cytosol, suggesting endocytic uptake (Supplementary Figure 1). The use of TEM to understand nanoparticle uptake only gives a snapshot of what is occurring in a cell at any given time. As such, the particles found in the cytosol could also have escaped from endosomes following active uptake. Studies in a macrophage cell line have demonstrated that amine PS are internalized by active processes and can enter the cytosol *via* lysosomal rupture.[32] Thus, it is important to also investigate pathways of nanoparticle uptake by functional, mechanistic methods also.

In addition to nanoparticle uptake, we also observed translocation across the epithelial monolayer. In order to rule out paracellular translocation, transepithelial electrical resistance (TEER) was monitored during the exposure period. Confluent monolayers of TT1 cells exhibited a TEER of 53.67Ω/cm^2 ± 1.03 which

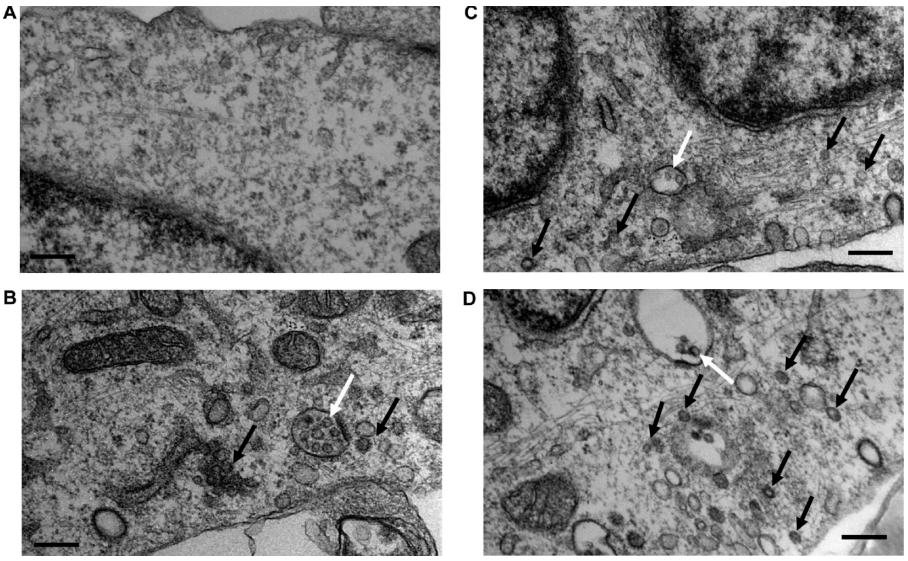

Figure 4. Intracellular distribution and translocation of internalized nanoparticles. (A) TT1 cells that were not exposed to nanoparticles; the endosomes and intracellular structures are relatively few and do not exhibit the dimensions of the nanoparticles used in this study. In contrast, TT1 cells exposed to 50 nm unmodified PS (B), carboxyl PS (C), and amine PS (D) contain numerous large endosomes, and nanoparticles were found clustered within the cytoplasm (black arrows) and endosomes (white arrows). Scale bar = 200 nm.

did not change over the course of the exposure period (data not shown). This finding supported our TEM studies demonstrating that nanoparticles do not disrupt tight junctions and thus cannot pass between cells. Comparative quantification of nanoparticles in the apical extracellular, intracellular, and basal extracellular compartments (Figure 5) demonstrated that approximately 3% of 50 nm unmodified PS translocated across the epithelial monolayer after 24 h. Interestingly, significantly more carboxyl PS (8%, $P = 0.0022$) translocated across the membrane compared to unmodified PS. Due to the limits of detection of the analytical method used, a higher concentration of nanoparticles was required to measure particle translocation, such that amine PS induced cytotoxicity, as previously described by us;[18] thus it was not possible to quantify their translocation. In addition, due to the significantly lower uptake of 100 nm nanoparticles compared to 50 nm nanoparticles it was not possible to detect any significant translocation of these particles.

The relatively low proportion of translocated nanoparticles observed in our system is in keeping with previous *in vivo* studies of other nanoparticles. Studies investigating translocation of pulmonary-delivered gold nanoparticles in rodents have shown approximately 0.5−3% of nanoparticles translocate into circulation.[28,33] While our findings are higher than that observed in these studies it should be noted that our *in vitro* system is not as complex as the air/blood barrier; in the *in vivo* setting, once translocated through the epithelial layer, particles also need to be able to traverse the interstitium and vascular endothelial layer in order to enter the bloodstream. It has been shown that a significant proportion of nanoparticles that translocate across the

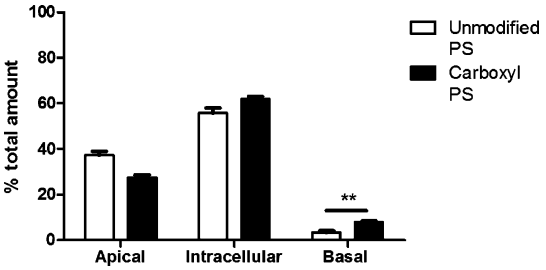

Figure 5. Translocation of internalized nanoparticles. Confluent monolayers of TT1 cells, grown on Transwell inserts, were exposed to 50 nm nanoparticles for 24 h. Following incubation, the relative amounts of nanoparticle in the apical, intracellular, and basal compartments were measured by fluorescent spectrophotometry. Results demonstrated that the majority of unmodified PS and carboxyl PS nanoparticles were found intracellularly. However, approximately 3% of unmodified PS translocated across the cell monolayer; significantly more (8%) carboxyl PS translocated compared to unmodified PS. Data expressed as the mean ± the standard deviation $n = 3$ experiments. $^{**}P = 0.0022$.

alveolar epithelial layer may become sequestered in the interstitium and the stromal cells found therein or be transported to lymph nodes *via* interstitial lymphatic drainage.[34] Indeed, the convective forces of lymphatic flow found in the interstitium *in vivo* which are absent in our model could have a significant impact on nanoparticle transport and warrant further investigation. The exact mechanisms underlying the basal release of particles from the epithelial monolayer are still unknown; however, it is likely that passive and active mechanisms may play a role. Previous studies have suggested that alveolar type I epithelial cells are important in macromolecular transport across the pulmonary epithelium *via* vesicles, which may be a likely route of translocation for endocytosed particles.[35]

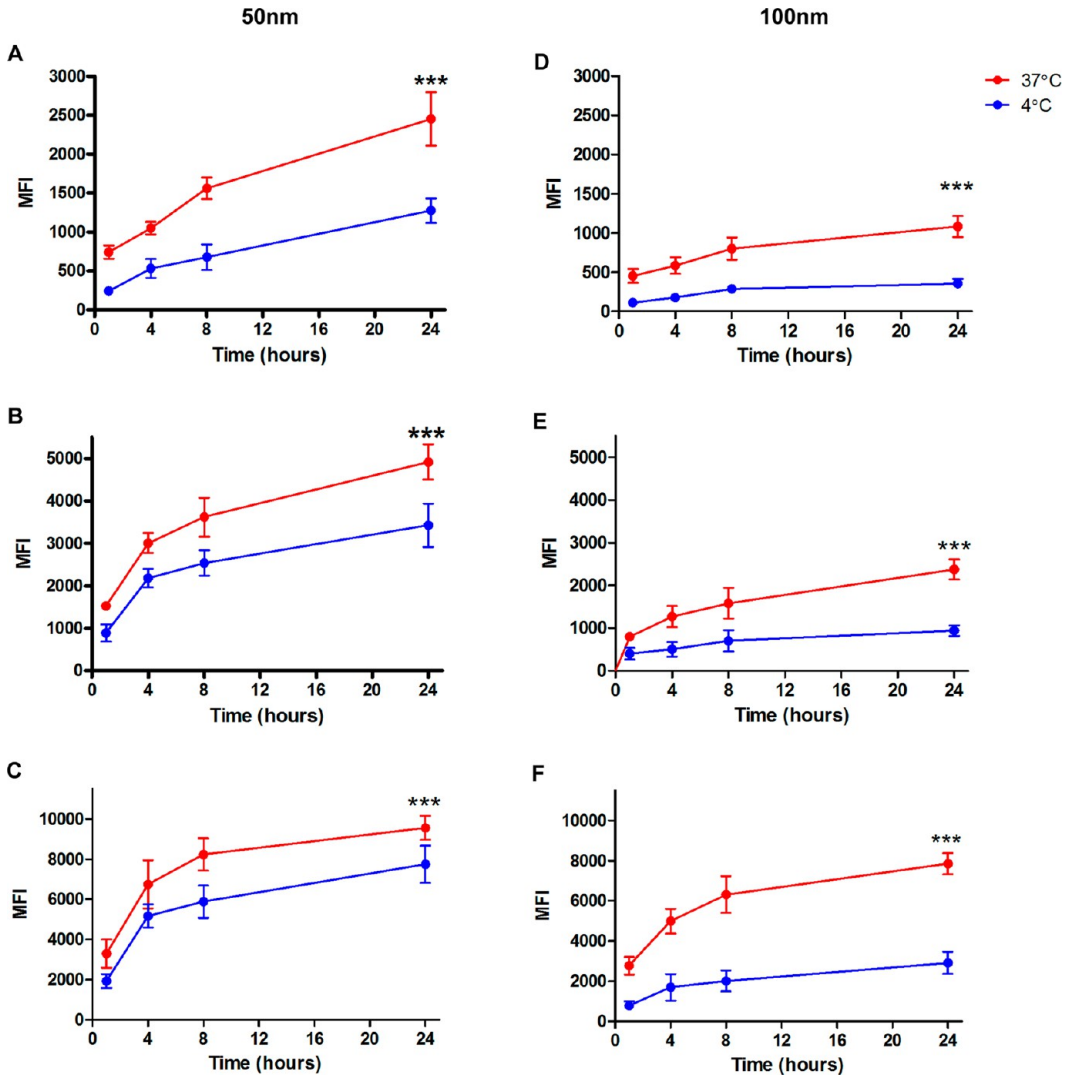

Figure 6. Temperature-dependent uptake of nanoparticles by TT1 cells. Confluent monolayers of TT1 cells were exposed to nanoparticles for up to 24 h at 37 or 4 °C. Uptake of all nanoparticles was significantly inhibited by cooling cells to 4 °C in order to inhibit active processes. However, uptake of 50 nm unmodified PS (A), unmodified PS (B), and amine PS (C) was inhibited significantly less by cooling cells compared to 100 nm unmodified PS (D), carboxyl PS (E), and amine PS (F). Data expressed as the mean ± the standard deviation $n = 4$ experiments. ***$P < 0.0001$.

Metabolic Inhibition of Nanoparticle Uptake. The presence of 50 nm nanoparticles free in the cytoplasm suggested that they might be able to enter the cell *via* direct interaction with the cell membrane and subsequent passive diffusion across the cell membrane. To investigate this, we compared uptake of nanoparticles at 37 °C with uptake at 4 °C, where all active processes such as endocytosis are inhibited. This showed that uptake of 50 and 100 nm of all modifications was significantly inhibited at 4 °C ($P < 0.0001$; Figure 6). After 4 h, uptake of 50 nm unmodified PS (Figure 6A) was inhibited by 49% whereas carboxyl PS (Figure 6B) and amine PS (Figure 6C) uptake was only inhibited by 27% and 23%, respectively. At the same time point, inhibition of uptake of 100 nm nanoparticles of all modifications was significantly greater than the equivalently surface-modified 50 nm nanoparticles ($P < 0.05$). Unlike the 50 nm particles, inhibition of uptake of all three types of 100 nm nanoparticles at 4 °C was similar, being 70%, 65% and 60% for unmodified PS, amine PS and carboxyl PS, respectively (Figure 6D–F). This supports our TEM observations showing that 100 nm nanoparticles enter largely *via* active endocytic pathways, whereas 50 nm nanoparticles, particularly those with surface modification, enter *via* (passive) diffusion across the cell membrane.

Clathrin- and Caveolin-Mediated Nanoparticle Endocytosis. To date, very little is known about the precise endocytic pathways that are present in noncancerous human alveolar epithelium, in particular alveolar type I epithelial cells. Many studies of alveolar epithelial endocytosis use pharmacological inhibitors such as chlorpromazine, cytochalasin D and nocodazole, which have a broad spectrum of biological effects, in *in vitro* models using rodent cells or human carcinoma-derived cell lines. We, and others, have previously shown that

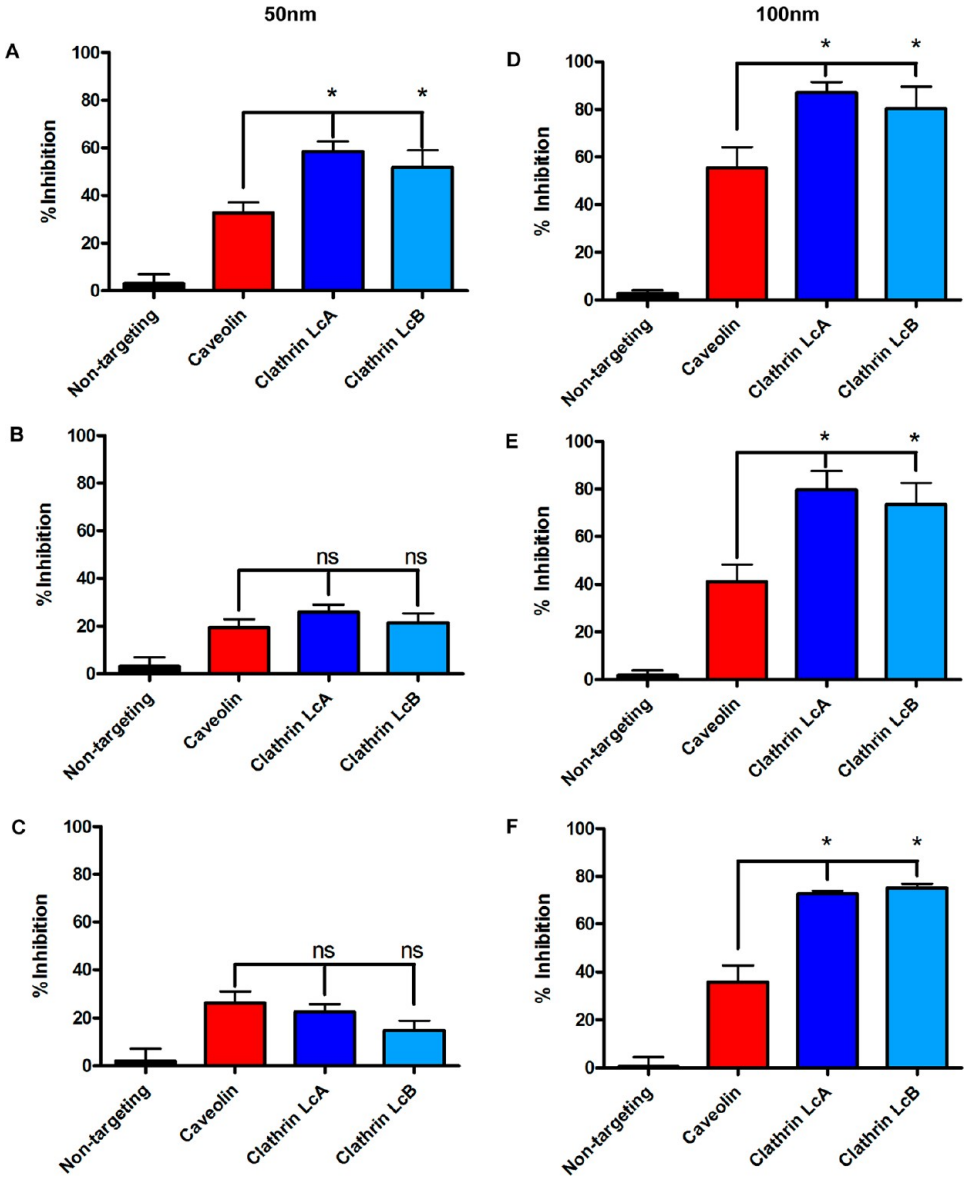

Figure 7. Inhibition of nanoparticle uptake by siRNA silencing of clathrin and caveolin protein expression. Caveolin and clathrin-mediated endocytosis was inhibited by silencing of caveolin-1 and clathrin LcA and LcB. Our results demonstrated that uptake of 50 nm unmodified PS (A) was inhibited significantly more than that of 50 nm carboxyl PS (B) and 50 nm amine PS (C). Interestingly, silencing of clathrin had a greater inhibitory effect on 50 nm unmodified PS uptake than silencing of caveolin-1, whereas for 50 nm carboxyl PS and amine PS there was no significant difference between the two pathways. Uptake of 100 nm nanoparticles was inhibited significantly more by endocytosis silencing compared to the equivalent 50 nm nanoparticles. Interestingly, the pattern of inhibition of uptake was similar for all three modifications; silencing of the clathrin endocytic pathway inhibited uptake of 100 nm unmodified PS (D) carboxyl PS (E) and amine PS (F) significantly more that silencing of the caveolin pathway. Data expressed as the mean ± the standard deviation $n = 4$ experiments. *$P = 0.05$.

human alveolar type I cells express caveolin-1,[7,15] indicating the presence of caveolin mediated endocytosis; however expression of clathrin proteins and the activity of the associated endocytosis pathway has not been conclusively demonstrated. To investigate the specific route of active, endosomal uptake of nanoparticles, we used siRNA to knockdown clathrin- (LcA 57% and LcB 43% knockdown), and caveolin- mediated (70% knockdown) endocytosis (Supplementary Figure 2, Supporting Information), two endocytic pathways we hypothesized would be present in human alveolar type I epithelial cells.

We discovered that knockdown of clathrin- and caveolin-mediated endocytosis inhibited uptake of 50 nm nanoparticles significantly less than uptake of 100 nm nanoparticles (Figure 7), supporting our hypothesis that 50 nm nanoparticles enter largely *via* nonendocytic pathways and that endosomal escape following active uptake is not the primary cause of cytosolic nanoparticles. Silencing of clathrin proteins inhibited TTI cell uptake of 50 nm unmodified PS (Figure 7A) significantly more (~55% vs ~20% and 23%, respectively, $P < 0.03$) than uptake of amine PS and carboxyl PS (Figure 7B and C, respectively),

complementing the temperature control study. Interestingly, silencing of caveolin-1 was significantly less effective at inhibiting uptake of 50 nm unmodified PS ($P = 0.05$), suggesting clathrin-mediated endocytosis is more important. In contrast, there was a similar effect of knockdown of caveolin and clathrin proteins on TTI cell uptake of 50 nm amine PS and carboxyl PS. There was no significant difference between knockdown of either of the clathrin proteins (LcA, LcB) in inhibition of particle uptake. Thus, these findings suggest that of the approximately 25% of 50 nm amine PS or carboxyl PS that are internalized by endocytosis, both clathrin- and caveolin-mediated pathways are important and both LcA and LcB clathrin proteins are required. In contrast, for a relatively greater proportion of 50 nm unmodified PS (approximately 50%), endocytosis is largely *via* a clathrin-mediated mechanism.

When these studies were repeated using 100 nm NPs (Figure 7D–F) the profile of inhibition was markedly different. Thus, knockdown of clathrin proteins inhibited uptake of all types of 100 nm NP to a similar level, approximately 80%, which was significantly greater than observed with 50 nm nanoparticles ($P = 0.05$). Silencing of caveolin-1 expression inhibited uptake of all three types of 100 nm particles significantly more than the equivalent 50 nm nanoparticles (approximately 2-fold; $P = 0.05$). In addition, inhibition of 100 nm unmodified PS (Figure 7D) uptake was significantly greater (1.5 fold; $P = 0.05$) than that of 100 nm amine PS and carboxyl PS (Figure 7E and F, respectively). Knockdown of clathrin proteins inhibited uptake of all three types of particle significantly more than knockdown of caveolin-1 (20–30% more; $P = 0.05$).

These studies are the first to use siRNA knockdown of endocytic proteins to investigate epithelial nanoparticle uptake and extend the findings of others using pharmacological inhibitors and other cell models of the alveolar epithelium. Investigating endocytosis pathways using *in vivo* models is difficult, particularly with siRNA; indeed, siRNA delivery to the lung for therapeutic purposes is an active field of research and is yet to yield successful results.[36] To date, we know of only one study where pharmacological inhibitors were used to inhibit endocytosis of proteins from the lung surface of rabbits.[37] In that study, it was shown that nocodazole and monensin inhibited epithelial uptake of albumin, which was also confirmed in *in vitro* cultures of rat ATII cells. Studies looking at the effect of size and charge of polystyrene nanoparticles on uptake by rat alveolar epithelial cells showed that 20 and 100 nm nanoparticles did not colocalize with clathrin or caveolin proteins and pharmacological inhibitors did not affect their uptake.[38] However, similar studies using canine kidney epithelial cells implicated clathrin-mediated endocytosis in uptake of the same nanoparticles, demonstrating that there are significant interspecies, and potentially anatomical, differences in particle translocation across the epithelial monolayers and highlight the importance of corroborating animal studies with studies using relevant human cells.

Thus, in human alveolar epithelial cells, we also believe that clathrin-dependent endocytosis is a significant process in the uptake of 100 nm nanoparticles, and this supports our previous findings using larger 200 nm nanoparticles;[39] however, in our studies, caveolin also plays a significant but lesser role. It is interesting that, despite similar levels of internalization into TTI cells, for unmodified PS, clathrin LcA and caveolin proteins are relatively more important, suggesting the involvement of specific molecular mechanisms that are related to surface charge differentiate the processes involved.

Lung Lining Liquid Potentiates Nanoparticle Uptake. Inhaled nanoparticles deposited in the alveolar region will first come into contact with a layer of lung lining liquid, an important component of which is pulmonary surfactant, before interacting with the underlying epithelium. Surfactant components are known to opsonize bacteria and may also bind to inhaled particles[40–42] and thus affect how a cell recognizes and interacts with a nanoparticle. To investigate this, we preincubated nanoparticles with human lung lining liquid (collected *via* bronchoalveolar lavage) for 30 min prior to cell exposure. Lavage fluid significantly potentiated the uptake of nanoparticles of all modifications ($p = 0.05$ Figure 8). Uptake of 50 nm carboxyl PS and amine PS was increased by approximately 40%, whereas uptake of 50 nm unmodified PS was increased by only 25% (Figure 8A). Similarly, uptake of 100 nm carboxyl PS and amine PS was increased by 50% and 42%, respectively, whereas uptake of unmodified PS was increased by 29% (Figure 8B).

These experiments demonstrate that the stimulatory effect of lung lining liquid on nanoparticle uptake is not size-dependent, but is charge-dependent, being most marked for amine PS and carboxyl PS (40–50% increase) compared to the unmodified PS (25–30% increase). This is the first study to investigate the role of human lung lining liquid on nanoparticle uptake by human alveolar epithelial cells and adds to previous studies showing the enhancing effect of non-native surfactants, such as bovine-derived surfactant, on nanoparticle uptake by carcinoma-derived cell lines.[43,44] The present study is of particular importance as the native lung lining liquid used contains the full spectrum of surfactant lipids and proteins whereas commercially available bovine- and porcine-derived surfactant preparations contain only phospholipids and surfactant proteins B and C at much lower levels than is found in native preparations.[45]

Surfactant Proteins Bind to the Nanoparticle Surface. The increased uptake of nanoparticles following preincubation with bronchoalveolar lavage fluid suggested

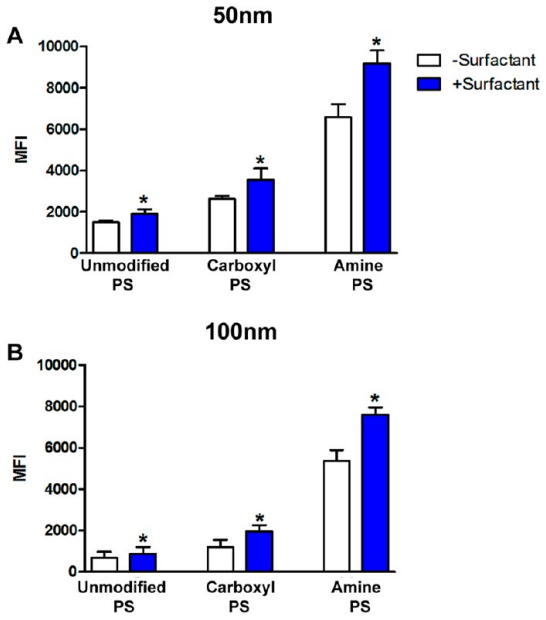

Figure 8. Lung lining liquid potentiates nanoparticle uptake. TT1 cells were exposed to nanoparticles in the absence or presence of surfactant for 4 h and uptake measured. Preincubation of 50 nm (A) and 100 nm (B) NPs with human lung lining liquid significantly increased uptake of all nanoparticles by human TT1 cells. Data expressed as mean ± standard deviation $n = 3$ experiments. *$P = 0.05$.

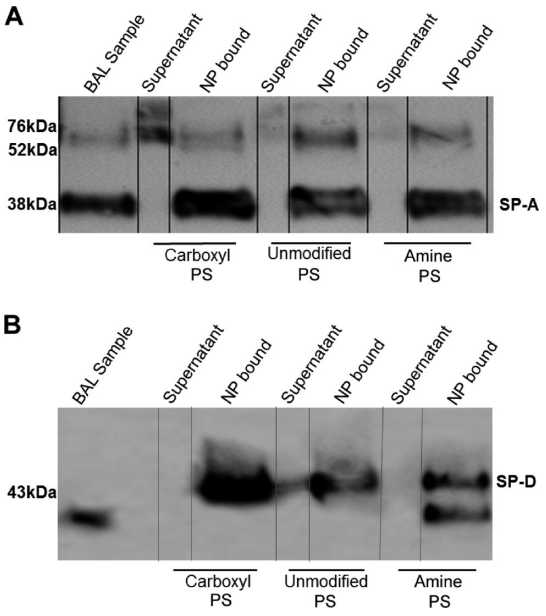

Figure 9. Surfactant proteins bind to the surface of nanoparticles. 50 nm nanoparticles were incubated with human lung lavage fluid for 1 h, and the presence of surfactant protein A (A) and surfactant protein D (B) bound to the nanoparticle surface and remaining in the supernatant was assessed by immunoblotting. Our results demonstrated that surfactant protein A and surfactant protein D both bound to the surface nanoparticles, regardless of surface modification. Immunoblots representative of three experiments.

that factors from the fluid were binding to the particle surface to promote uptake. Previous studies using animal-derived, isolated, or recombinant surfactant have demonstrated binding of surfactant proteins to a variety of nanoparticles.[46,47] However, to date, there have been no previous studies that have used total native human surfactant to investigate its adsorption to nanoparticles. Immunoblotting demonstrated that both SP-A (Figure 9A) and SP-D (Figure 9B) bound to the surface of nanoparticles. The surfactant proteins are c-type lectins that are critical in the host response to invading pathogens. Binding of the proteins to the microbe causes agglutination and marks the microbes for clearance. Studies have demonstrated that SP-A and SP-D bind to a number of cell surface receptors on macrophages and endothelial cells.[48] In addition, SP-A and SP-D are known to bind to CD14 and Toll-like receptors 2 and 4[49,50] which we have previously shown to be expressed on alveolar type I cells;[23] it is possible that interaction with cell surface receptors such as these may facilitate particle uptake and requires further investigation.

CONCLUSION

In this study we have systematically investigated the effect of nanoparticle size and surface modification on the interaction of nanoparticles with human alveolar epithelial cells and pulmonary surfactant; these novel mechanistic studies suggest specific patterns of particle behavior with pulmonary surfactant and epithelial cells based on the physicochemical properties of nanoparticles, and give a unique insight into how particle characteristics could be manipulated to enhance uptake by the respiratory epithelium and improve drug delivery in the human lung. The use of model polystyrene nanoparticles in this study allows us to hypothesize how fundamental properties may affect degree and route of uptake of nanoparticles; however, it is important that uptake of nanoparticles is assessed on an individual basis as even small changes in size and charge, along with particle composition could alter the end points measured in this study. Of particular importance to the field of drug delivery is the observation of significant uptake of carboxyl-modified nanoparticles and their subsequent translocation through the monolayer. In conjunction with our previous findings of cytotoxicity associated with positively charged particles, we suggest that the use of negatively charged nanoparticles, rather than the more commonly investigated positively charged particles, will ensure effective uptake in to epithelial cells without any associated toxicity.

Thus, in light of the rapid development of nanoparticles for commercial and therapeutic applications, this study highlights the importance of investigating uptake of emerging nanodrugs to observe whether these patterns are true for other formats. In addition, it will be important to determine how internalized particles are processed; if they are targeted to lysosomes for degradation or are small enough to enter the nucleus

or interact with other cellular organelles such as mitochondria, how will this affect drug efficacy or potential cytotoxicity? These factors will clearly need to be addressed on a particle by particle basis but should offer some exciting insights for future technologies.

METHODS

Culture of Immortalized ATI Cells. We have created a unique immortalized human ATI cell line,[15] using previously published techniques,[51] that shows the same characteristics as ATI cells *in vivo*. Stocks of TT1 (immortalized ATI) cells were plated in DCCM-1 media (Cadama, UK) containing 10% NCS and 1% PSG at a density of 0.5×10^6/well in a 24 well plate. Cells reached confluency within 48 h. Prior to experiments, cells were serum starved for 24 h.

Isolation of Primary Human Type II Epithelial Cells. ATII cells were isolated from lung tissue as previously described.[52] Cells were suspended in DCCM-1 media (Cadama, UK) containing 10% NCS and 1% penicillin/streptomycin/glutamine (PSG; Invitrogen, UK) and seeded at 0.5×10^6 ATII cells per well in 24 well plates coated with 1% type I collagen solution (PureCol, Netherlands). By 48 h, cells were confluent and had a purity of >95% as previously demonstrated.[53] These cells have been thoroughly characterized using electron microscopy, which shows that the cells are cuboidal in morphology, have surfactant-containing lamellar bodies, tight junctions, and microvilli. Furthermore, they stain positively for the ATII cell marker alkaline phosphatase and express surfactant proteins A and C and maintain their phenotype for up to 6 days.[52,53] Prior to experiments, cells were serum starved for 24 h.

Nanoparticle Exposure. Confluent monolayers of TT1 and ATII cells were exposed to 50 or 100 nm fluorescently labeled polystyrene nanoparticles (Bangs Laboratories, USA) that were unmodified, carboxyl-modified or amine-modified. Previous studies in our laboratory have confirmed the physicochemical properties of these nanoparticles in the media used in this study and demonstrated that concentrations above 50 μg/mL of 50 nm nanoparticles may induce toxicity,[18] thus for these studies 40 μg/mL was used. Particles were suspended in serum-free media and sonicated in an ultrasonic water bath for 1 min. Cells were then exposed for up to 4 h; at each time point, the media was removed and the wells washed with Dulbecco's phosphate buffered saline (DPBS) to remove any particles that had not been internalized.

Measurement of Nanoparticle Uptake. Cellular uptake was visualized using fluorescent microscopy. To rule out residual extracellular nanoparticles confounding quantification of nanoparticle uptake, fluorescence was measured in the presence of Trypan blue, a known quencher of FITC.[54,55] The presence of Trypan Blue did not significantly alter measurements, confirming there were no extracellular nanoparticles remaining. Simple PCI image analysis software (Digital Pixel, UK) was used to measure the mean fluorescent intensity (MFI) of five randomly selected fields of view per exposure condition as an index of the degree of cellular uptake. In order to standardize the fluorescent signal of the nanoparticles, prior to image capture the exposure time, and gain (detector sensitivity) of the system was adjusted so that the same MFI was emitted by identical concentrations of each of the nanoparticles.

Electron Microscopy of Cellular Uptake. To visualize the uptake and cellular fate of nanoparticles, ATI cells were exposed to 50 and 100 nm unmodified, carboxyl-modified, and amine-modified polystyrene nanoparticles as before. Following exposure, cells were rinsed with PBS and fixed with 2.5% glutaraldehyde for 2 h. The samples were postfixed in 1% osmium tetraoxide for 15–30 min. Samples were then washed with distilled water and dehydrated, in 70% ethanol (1×), 90% ethanol (1×), and 100% ethanol (3×), respectively, for 15 min for each step at room temperature. To maintain the integrity of the monolayer and prevent shrinkage, cells were incubated with Araldite in ethanol 50% v/v for 15 min. This solution assists the infiltration of Araldite in to the cells. After 15 min, the solution was removed and 100% Araldite added for a further 15 min. Following this, the solution was removed and an embedding capsule containing 100% Araldite was placed on top of the monolayer and then placed in an oven at 60 °C for 48 h to polymerize. The capsule embedded cell monolayer was cut on a microtome into ultrathin sections, 0.05–0.20 μm. Sections were stained with 1.5% uranium acetate and 5% lead citrate before viewing under transmission electron microscope (TEM).

Quantification of Nanoparticle Translocation. To determine whether nanoparticles could translocate across intact TT1 cell monolayers, TT1 cells were grown on Corning Costar Transwell inserts. Confluent cells were serum starved for 24 h before addition of 50 μg/mL of 50 nm nanoparticles for 24 h. Following incubation, cell culture media from the apical and basal sides of the cells was collected and the cell monolayer lysed with CelLytic M (Sigma-Aldrich, UK) and collected for analysis. The relative proportion of the nanoparticles in each compartment was measured using a spectrofluorimeter.

Energy Requirement for Cellular Uptake. To determine whether internalization of nanoparticles was active or passive, cells were either maintained at 37 °C, where energy requiring mechanisms will function normally, or at 4 °C, where all energy requiring mechanisms are inhibited for 1 h before nanoparticle exposure and during exposure. Cells were exposed to nanoparticles for up to 24 h and processed for image analysis as before.

siRNA Knockdown of Endocytic Proteins. Clathrin- and caveolin-mediated endocytosis were inhibited using siRNA knockdown of proteins integral to each of the pathways, clathrin LcA, clathrin LcB, and caveolin-1 (Supporting Information). ATI cells were seeded in Accell delivery media (Thermo Scientific, UK) containing the relevant siRNA, or negative control (1 μM final concentration; Thermo Scientific) was added to the cells. Cells were incubated for 72 h, during which time cells reached confluency and knockdown of target proteins was achieved.

Following knockdown of proteins, cells were exposed to 40 μg/mL of 50 or 100 nm nanoparticles of each modification for 4 h, and cellular uptake was measured as before.

Effect of Surfactant Binding. Nanoparticles were suspended in human bronchoalveolar lavage fluid (0.9 mg/mL protein content) at a stock concentration of 2 mg/mL for 1 h prior to being diluted down to a working concentration of 40 μg/mL. Cells were exposed for 4 h and imaged as above.

Determining Bound Surfactant Proteins. Surfactant-bound proteins were detected using an adapted previously described protocol.[56] Nanoparticles were incubated in concentrated BAL as before. Samples were then centrifuged at 5000*g* for 10 min to separate NPs and bound components from the unbound solution. The supernatant was aspirated and saved, while the pellet was washed in PBS and centrifuged three times to remove any unbound proteins. NuPAGE LDS sample buffer (Invitrogen, UK) was then added to the saved supernatant and resuspended pellet, and the samples were heated at 80 °C for 10 min. Samples were then loaded into 4–12% NuPAGE Bis-Tris gels. Gels were run in NuPAGE MOPS SDS running buffer, and protein bands were then transferred to a polyvinylidene difluoride (PVDF) membrane. Membranes were then washed and blocked for 1 h in TBST containing 5% BSA. Membranes were probed for SP-A using a polyclonal rabbit antibody (1 μg/mL; Abcam, UK) or SP-D using a monoclonal mouse antibody (0.3 μg/mL, Abcam).

Statistical Analyses. All statistical comparisons were selected *a priori*, and Gaussian distribution was not assumed. To determine the statistical significance of nanoparticle uptake over time, Kruskal–Wallis one-way analysis of variance (ANOVA) was used. A two-way ANOVA was used to compare the time-dependent uptake of nanoparticles of differing size and surface modification and to compare the effect of temperature on time-dependent uptake. Comparison of translocation of nanoparticles of differing surface modification, effect of siRNA

silencing of proteins on nanoparticle uptake, and effect of pretreatment with lung lining liquid was done using one-tailed Mann−Whitney U analysis.

Conflict of Interest: The authors declare no competing financial interest.

Supporting Information Available: Methods of measurement of clathrin and caveolin expression and supplementary figures showing TEM images of 100 nm nanoparticle uptake by TT1 cells and siRNA knockdown of expression of clathrin and caveolin proteins. This material is available free of charge *via* the Internet at http://pubs.acs.org.

Acknowledgment. This work was carried out as part of the MRC-PHE Centre for Environment and Health, supported jointly by the Medical Research Council and Public Health England. This work was also supported by the NIHR Respiratory Disease Biomedical Research Unit at the Royal Brompton and Harefield NHS Foundation Trust and Imperial College London. Support was provided by the Department for Environment, Fisheries and Rural Affairs (T.D.T., A.J.T.), Engineering and Physical Sciences Research Council (A.J.T.), NIEHS (No. U19ES019536, T.D.T., A.J.T.) and Leverhulme Trust (T.D.T., P.R.).

REFERENCES AND NOTES

1. The Project on Emerging Nanotechnologies: Consumer Product Inventory. The Woodrow Wilson International Center for Scholars. 2014. http://www.nanotechproject.org/cpi (accessed Oct 26, 2014).
2. Peer, D.; Karp, J. M.; Hong, S.; Farokhzad, O. C.; Margalit, R.; Langer, R. Nanocarriers As an Emerging Platform for Cancer Therapy. *Nat. Nano.* **2007**, *2*, 751–760.
3. Davis, M. E.; Zuckerman, J. E.; Choi, C. H.; Seligson, D.; Tolcher, A.; Alabi, C. A.; Yen, Y.; Heidel, J. D.; Ribas, A. Evidence of RNAi in Humans from Systemically Administered siRNA *Via* Targeted Nanoparticles. *Nature* **2010**, *464*, 1067–1070.
4. Kurmi, B. D.; Kayat, J.; Gajbhiye, V.; Tekade, R. K.; Jain, N. K. Micro- and Nanocarrier-mediated Lung Targeting. *Expert. Opin. Drug Delivery* **2010**, *7*, 781–794.
5. Thorley, A. J.; Tetley, T. D. New Perspectives in Nanomedicine. *Pharmacol. Ther.* **2013**, *140*, 176–185.
6. Oberdorster, G.; Oberdorster, E.; Oberdorster, J. Nanotoxicology: An Emerging Discipline Evolving from Studies of Ultrafine Particles. *Environ. Health Perspect.* **2005**, *113*, 823–839.
7. Wang, S.; Singh, R. D.; Godin, L.; Pagano, R. E.; Hubmayr, R. D. Endocytic Response of Type I Alveolar Epithelial Cells to Hypertonic Stress. *Am. J. Physiol. Lung Cell Mol. Physiol.* **2011**, *300*, L560–L568.
8. Williams, M. C. Alveolar Type I Cells: Molecular Phenotype and Development. *Annu. Rev. Physiol.* **2003**, *65*, 669–695.
9. Kendall, M.; Guntern, J.; Lockyer, N. P.; Jones, F. H.; Hutton, B. M.; Lippman, M.; Tetley, T. D. Urban PM2.5 Surface Chemistry and Interactions with Bronchoalveolar Lavage Fluid. *Inhal. Toxicol.* **2004**, *16*, 115–129.
10. Schurch, S.; Gehr, P.; Im Hof, V.; Geiser, M.; Green, F. Surfactant Displaces Particles toward the Epithelium in Airways and Alveoli. *Respir. Physiol.* **1990**, *80*, 17–32.
11. Fisher, A. B.; Dodia, C.; Ruckert, P.; Tao, J. Q.; Bates, S. R. Pathway to Lamellar Bodies for Surfactant Protein A. *Am. J. Physiol. Lung Cell Mol. Physiol.* **2010**, *299*, L51–L58.
12. Griese, M.; Beck, J.; Feuerhake, F. Surfactant Lipid Uptake and Metabolism by Neonatal and Adult Type II Pneumocytes. *Am. J. Physiol. Lung Cell Mol. Physiol.* **1999**, *277*, L901–L909.
13. Takenaka, S.; Karg, E.; Kreyling, W. G.; Lentner, B.; Möller, W.; Behnke-Semmler, M.; Jennen, L.; Walch, A.; Michalke, B.; Schramel, P.; *et al.* Distribution Pattern of Inhaled Ultrafine Gold Particles in the Rat Lung. *Inhal. Toxicol.* **2006**, *18*, 733–740.
14. Sung, J. H.; Ji, J. H.; Park, J. D.; Yun, J. U.; Kim, D. S.; Jeon, K. Sf.; Song, M. Y.; Jeong, J.; Han, B. S.; Han, J. H.; *et al.* Subchronic Inhalation Toxicity of Silver Nanoparticles. *Toxicol. Sci.* **2008**, *108*, 452–461.
15. Kemp, S. J.; Thorley, A. J.; Gorelik, J.; Seckl, M. J.; O'Hare, M. J.; Arcaro, A.; Korchev, Y.; Goldstraw, P.; Tetley, T. D. Immortalization of Human Alveolar Epithelial Cells to Investigate Nanoparticle Uptake. *Am. J. Respir. Cell Mol. Biol.* **2008**, *39*, 591–597.
16. dos Santos, T.; Varela, J.; Lynch, I.; Salvati, A.; Dawson, K. A. Effects of Transport Inhibitors on the Cellular Uptake of Carboxylated Polystyrene Nanoparticles in Different Cell Lines. *PLoS One* **2011**, *6*, e24438.
17. Vercauteren, D.; Vandenbroucke, R. E.; Jones, A. T.; Rejman, J.; Demeester, J.; De Smedt, S. C.; Sanders, N. N.; Braeckmans, K. The Use of Inhibitors to Study Endocytic Pathways of Gene Carriers: Optimization and Pitfalls. *Mol. Ther.* **2010**, *18*, 561–569.
18. Ruenraroengsak, P.; Novak, P.; Berhanu, D.; Thorley, A. J.; Valsami-Jones, E.; Gorelik, J.; Korchev, Y. E.; Tetley, T. D. Respiratory Epithelial Cytotoxicity and Membrane Damage (Holes) Caused by Amine-modified Nanoparticles. *Nanotoxicology* **2012**, *6*, 94–108.
19. Grabowski, N.; Hillaireau, H.; Vergnaud, J.; Santiago, L. A.; Kerdine-Romer, S.; Pallardy, M.; Tsapis, N.; Fattal, E. Toxicity of Surface-modified PLGA Nanoparticles toward Lung Alveolar Epithelial Cells. *Int. J. Pharm.* **2013**, *454*, 686–694.
20. Varela, J. A.; Bexiga, M. G.; Aberg, C.; Simpson, J. C.; Dawson, K. A. Quantifying Size-Dependent Interactions between Fluorescently Labeled Polystyrene Nanoparticles and Mammalian Cells. *J. Nanobiotechnol.* **2012**, *10*, 39.
21. Dorney, J.; Bonnier, F.; Garcia, A.; Casey, A.; Chambers, G.; Byrne, H. J. Identifying and Localizing Intracellular Nanoparticles Using Raman Spectroscopy. *Analyst* **2012**, *137*, 1111–1119.
22. Swain, R. J.; Kemp, S. J.; Goldstraw, P.; Tetley, T. D.; Stevens, M. M. Assessment of Cell Line Models of Primary Human Cells by Raman Spectral Phenotyping. *Biophys. J.* **2010**, *98*, 1703–1711.
23. Thorley, A. J.; Grandolfo, D.; Lim, E.; Goldstraw, P.; Young, A.; Tetley, T. D. Innate Immune Responses to Bacterial Ligands in the Peripheral Human Lung - Role of Alveolar Epithelial TLR Expression and Signalling. *PLoS One* **2011**, *6*, e21827.
24. Gao, H.; Shi, W.; Freund, L. B. Mechanics of Receptor-mediated Endocytosis. *Proc. Natl. Acad. Sci. U.S.A.* **2005**, *102*, 9469–9474.
25. Limbach, L. K.; Li, Y.; Grass, R. N.; Brunner, T. J.; Hintermann, M. A.; Muller, M.; Gunther, D.; Stark, W. J. Oxide Nanoparticle Uptake in Human Lung Fibroblasts: Effects of Particle Size, Agglomeration, and Diffusion at Low Concentrations. *Environ. Sci. Technol.* **2005**, *39*, 9370–9376.
26. Herzog, F.; Loza, K.; Balog, S.; Clift, M. J.; Epple, M.; Gehr, P.; Petri-Fink, A.; Rothen-Rutishauser, B. Mimicking Exposures to Acute and Lifetime Concentrations of Inhaled Silver Nanoparticles by Two Different *In Vitro* Approaches. *Beilstein J. Nanotechnol.* **2014**, *5*, 1357–1370.
27. Sarlo, K.; Blackburn, K. L.; Clark, E. D.; Grothaus, J.; Chaney, J.; Neu, S.; Flood, J.; Abbott, D.; Bohne, C.; Casey, K.; *et al.* Tissue Distribution of 20nm, 100nm and 1000nm Fluorescent Polystyrene Latex Nanospheres Following Acute Systemic or Acute and Repeat Airway Exposure in the Rat. *Toxicology* **2009**, *263*, 117–126.
28. Schleh, C.; Holzwarth, U.; Hirn, S.; Wenk, A.; Simonelli, F.; Schaffler, M.; Möller, W.; Gibson, N.; Kreyling, W. G. Biodistribution of Inhaled Gold Nanoparticles in Mice and the Influence of Surfactant Protein D. *J. Aerosol Med. Pulm. Drug Delivery* **2012**, *26*, 24–30.
29. Naota, M.; Shimada, A.; Morita, T.; Inoue, K.; Takano, H. Translocation Pathway of the Intratracheally Instilled C60 Fullerene from the Lung into the Blood Circulation in the Mouse: Possible Association of Diffusion and Caveolae-mediated Pinocytosis. *Toxicol. Pathol.* **2009**, *37*, 456–462.
30. Liu, J.; Gong, T.; Fu, H.; Wang, C.; Wang, X.; Chen, Q.; Zhang, Q.; He, Q.; Zhang, Z. Solid Lipid Nanoparticles for Pulmonary Delivery of Insulin. *Int. J. Pharm.* **2008**, *356*, 333–344.
31. Neumiller, J. J.; Campbell, R. K. Technosphere Insulin: An Inhaled Prandial Insulin Product. *BioDrugs* **2010**, *24*, 165–172.

32. Xia, T.; Kovochich, M.; Liong, M.; Zink, J. I.; Nel, A. E. Cationic Polystyrene Nanosphere Toxicity Depends on Cell-Specific Endocytic and Mitochondrial Injury Pathways. *ACS Nano* **2008**, *2*, 85–96.
33. Lipka, J.; Semmler-Behnke, M.; Sperling, R. A.; Wenk, A.; Takenaka, S.; Schleh, C.; Kissel, T.; Parak, W. J.; Kreyling, W. G. Biodistribution of PEG-Modified Gold Nanoparticles Following Intratracheal Instillation and Intravenous Injection. *Biomaterials* **2010**, *31*, 6574–6581.
34. Porter, D. W.; Wu, N.; Hubbs, A. F.; Mercer, R. R.; Funk, K.; Meng, F.; Li, J.; Wolfarth, M. G.; Battelli, L.; Friend, S.; *et al.* Differential Mouse Pulmonary Dose and Time Course Responses to Titanium Dioxide Nanospheres and Nanobelts. *Toxicol. Sci.* **2013**, *131*, 179–193.
35. Kim, K. J.; Malik, A. B. Protein Transport across the Lung Epithelial Barrier. *Am. J. Physiol. Lung Cell. Mol. Physiol.* **2003**, *284*, L247–L259.
36. Merkel, O. M.; Rubinstein, I.; Kissel, T. siRNA Delivery to the Lung: What's New? *Adv. Drug Delivery Rev.* **2014**, *75*, 112–128.
37. Hastings, R. H.; Wright, J. R.; Albertine, K. H.; Ciriales, R.; Matthay, M. A. Effect of Endocytosis Inhibitors on Alveolar Clearance of Albumin, Immunoglobulin G, and SP-A in Rabbits. *Am. J. Physiol.* **1994**, *266*, L544–552.
38. Yacobi, N. R.; Malmstadt, N.; Fazlollahi, F.; DeMaio, L.; Marchelletta, R.; Hamm-Alvarez, S. F.; Borok, Z.; Kim, K. J.; Crandall, E. D. Mechanisms of Alveolar Epithelial Translocation of a Defined Population of Nanoparticles. *Am. J. Respir. Cell Mol. Biol.* **2010**, *42*, 604–614.
39. Novak, P.; Shevchuk, A.; Ruenraroengsak, P.; Miragoli, M.; Thorley, A. J.; Klenerman, D.; Lab, M. J.; Tetley, T. D.; Gorelik, J.; Korchev, Y. E. Imaging Single Nanoparticle Interactions with Human Lung Cells Using Fast Ion Conductance Microscopy. *Nano Lett.* **2014**, *14*, 1202–1207.
40. Leo, B. F.; Chen, S.; Kyo, Y.; Herpoldt, K. L.; Terrill, N. J.; Dunlop, I. E.; McPhail, D. S.; Shaffer, M. S.; Schwander, S.; Gow, A.; *et al.* The Stability of Silver Nanoparticles in a Model of Pulmonary Surfactant. *Environ. Sci. Technol.* **2013**, *47*, 11232–11240.
41. Gasser, M.; Wick, P.; Clift, M. J.; Blank, F.; Diener, L.; Yan, B.; Gehr, P.; Krug, H. F.; Rothen-Rutishauser, B. Pulmonary Surfactant Coating of Multi-Walled Carbon Nanotubes (MWCNTs) Influences their Oxidative and Pro-Inflammatory Potential *In Vitro*. *Part. Fibre Toxicol.* **2012**, *9*, 17.
42. Ruge, C. A.; Schaefer, U. F.; Herrmann, J.; Kirch, J.; Cañadas, O.; Echaide, M.; Perez-Gil, J.; Casals, C.; Müller, R.; Lehr, C. M. The Interplay of Lung Surfactant Proteins and Lipids Assimilates the Macrophage Clearance of Nanoparticles. *PLoS One* **2012**, *7*, e40775.
43. Benfer, M.; Kissel, T. Cellular Uptake Mechanism and Knockdown Activity of siRNA-Loaded Biodegradable DEAPA-PVA-g-PLGA Nanoparticles. *Eur. J. Pharm. Biopharm.* **2012**, *80*, 247–256.
44. Nguyen, J.; Reul, R.; Betz, T.; Dayyoub, E.; Schmehl, T.; Gessler, T.; Bakowsky, U.; Seeger, W.; Kissel, T. Nanocomposites of Lung Surfactant and Biodegradable Cationic Nanoparticles Improve Transfection Efficiency to Lung Cells. *J. Controlled Release* **2009**, *140*, 47–54.
45. Bernhard, W.; Mottaghian, J.; Gebert, A.; Rau, G. A.; von der Hardt, H.; Poets, C. F. Commercial *Versus* Native Surfactants. *Am. J. Respir. Crit. Care Med.* **2000**, *162*, 1524–1533.
46. Schulze, C.; Schaefer, U. F.; Ruge, C. A.; Wohlleben, W.; Lehr, C. M. Interaction of Metal Oxide Nanoparticles with Lung Surfactant Protein A. *Eur. J. Pharm. Biopharm.* **2011**, *77*, 376–383.
47. Kendall, M.; Ding, P.; Mackay, R. M.; Deb, R.; McKenzie, Z.; Kendall, K.; Madsen, J.; Clark, H. Surfactant Protein D (SP-D) Alters Cellular Uptake of Particles and Nanoparticles. *Nanotoxicology* **2012**, *7*, 963–973.
48. Kishore, U.; Greenhough, T. J.; Waters, P.; Shrive, A. K.; Ghai, R.; Kamran, M. F.; Bernal, A. L.; Reid, K. B. M.; Madan, T.; Chakraborty, T. Surfactant Proteins SP-A and SP-D: Structure, Function and Receptors. *Mol. Immunol.* **2006**, *43*, 1293–1315.
49. Sano, H.; Chiba, H.; Iwaki, D.; Sohma, H.; Voelker, D. R.; Kuroki, Y. Surfactant Proteins A and D Bind CD14 by Different Mechanisms. *J. Biol. Chem.* **2000**, *275*, 22442–22451.
50. Ohya, M.; Nishitani, C.; Sano, H.; Yamada, C.; Mitsuzawa, H.; Shimizu, T.; Saito, T.; Smith, K.; Crouch, E.; Kuroki, Y. Human Pulmonary Surfactant Protein D Binds the Extracellular Domains of Toll-like Receptors 2 and 4 Through the Carbohydrate Recognition Domain by a Mechanism Different from its Binding to Phosphatidylinositol and Lipopolysaccharide. *Biochemistry* **2006**, *45*, 8657–8664.
51. O'Hare, M. J.; Bond, J.; Clarke, C.; Takeuchi, Y.; Atherton, A. J.; Berry, C.; Moody, J.; Silver, A. R. J.; Davies, D. C.; Alsop, A. E.; *et al.* Conditional Immortalization of Freshly Isolated Human Mammary Fibroblasts and Endothelial Cells. *Proc. Natl. Acad. Sci. U.S.A.* **2001**, *98*, 646–651.
52. Witherden, I. R.; Tetley, T. D. Isolation and Culture of Human Alveolar Type II Pneumocytes. In *Human Airway Inflammation; Sampling Techniques and Analytical Protocols*; Rogers, D. F., Donnelly, L. D., Ed.; Humana Press: Totowa, 2001; pp 137−146.
53. Witherden, I. R.; Vanden Bon, E. J.; Goldstraw, P.; Ratcliffe, C.; Pastorino, U.; Tetley, T. D. Primary Human Alveolar Type II Epithelial Cell Chemokine Release: Effects of Cigarette Smoke and Neutrophil Elastase. *Am. J. Respir. Cell Mol. Biol.* **2004**, *30*, 500–509.
54. Vranic, S.; Boggetto, N.; Contremoulins, V.; Mornet, S.; Reinhardt, N.; Marano, F.; Baeza-Squiban, A.; Boland, S. Deciphering the Mechanisms of Cellular Uptake of Engineered Nanoparticles by Accurate Evaluation of Internalization Using Imaging Flow Cytometry. *Part. Fibre Toxicol.* **2013**, *10*, 2.
55. Endres, T.; Zheng, M.; Klç, A.; Turowska, A.; Beck-Broichsitter, M.; Renz, H.; Merkel, O. M.; Kissel, T. Amphiphilic Biodegradable PEG-PCL-PEI Triblock Copolymers for FRET-Capable *In Vitro* and *In Vivo* Delivery of siRNA and Quantum Dots. *Mol. Pharmaceutics* **2014**, *11*, 1273–1281.
56. Lundqvist, M.; Stigler, J.; Elia, G.; Lynch, I.; Cedervall, T.; Dawson, K. A. Nanoparticle Size and Surface Properties Determine the Protein Corona with Possible Implications for Biological Impacts. *Proc. Natl. Acad. Sci. U.S.A.* **2008**, *105*, 14265–14270.